

IMPACT OF THE TUMBLING RATE ON THE PERFORMANCES OF A CW LASER DEFLECTOR

Nicolas Thiry¹, M. Vasile¹, University of Strathclyde, Glasgow, 75 Montrose Street G1 1XJ United Kingdom; nicolas.thiry@strath.ac.uk

Keywords: Asteroid, laser, ablation, deflection, de-tumbling

Abstract: Owing to their ability to move a target in space without requiring propellant, laser-based deflection methods have gained attention among the research community in the recent years. With laser ablation, the vaporized material is used to push the target itself allowing for a significant reduction in the mass requirements for an asteroid deflection mission. Specifically, this paper addresses the impact of the tumbling motion of the target on the efficiency of a deflection method using a CW laser. We developed an analytical steady-state model based on energetic considerations in order to predict the efficiency range theoretically allowed when the target is not moving with respect to the laser beam. A numerical model was then developed to solve the transient heat equation in presence of vaporization and melting. The comparison between the numerical results and the analytical predictions allow us to draw interesting conclusion regarding the applicability range of a given laser-based deflection system.

Introduction:

Deflection methods are traditionally divided into two main categories depending on whether or not the modification of the orbital trajectory can be done in a quasi-instantaneous way or need to be acted over a longer period of time by slowly pushing the target away of its collision course. Impulsive techniques produce an impulsive energy transfer by exploding for example a nuclear device (nuclear interceptor) or crashing a massive spacecraft (kinetic impactor) to modify the velocity of the asteroid and thus its orbital trajectory. Slow-push methods on the other hand allow for a more controllable deflection manoeuvre by exerting a small force on the asteroid over an extended period of time. This ability to manipulate precisely the trajectory of an asteroid by contrast with the relatively crude approach offered by impulsive methods explains by itself the growing interest for these slow-push methods. Over the past years many concepts have been proposed and studied with various degrees of accuracy. Among these methods, laser ablation opens a very promising path of research. Indeed, in most cases, the efficiency of the deflection technique is eventually limited by the amount of propellant available from the beginning of the mission. For methods using laser ablation, this limitation is removed as the vaporized asteroid material is used to propel itself. Thanks to this, the mass allocation can be shifted from the propellant to the power systems. Several mission concepts using laser ablation as a deflection



Figure 1: The Laser Bees project

method have been investigated in the past by the University of Strathclyde and are worthwhile mentioning. The Light Touch concept proposed by [1] aims at changing the orbital velocity of a 4 m diameter, 130 tons asteroid by 1 m/s in less than 3 years using a 453kgs spacecraft. The study was performed in cooperation with the University of Southampton, Astrium Ltd and GMV-SKY as an answer the SysNova challenge, an ESA initiative. Another approach investigated by [2] has been the use of solar concentrators to power a laser-based deflector. While it may sound curious to convert solar power into another form of optical power, the higher energy density provided by the laser beam is required to reach a sufficiently high temperature to enable the vaporization process. Supported by the planetary society, the laser bees project investigates the use of a swarm of solar-pumped lasers. Flying in formation around the target asteroid, the combination of multiple beams allow to produce a higher thrust without requiring the use of a nuclear reactor. In addition, the swarm offers redundancy in the case of failure of a single spacecraft. In this paper, we attempt to address an important issues which has remained unanswered by previous studies: the impact of the tumbling motion of the target on the efficiency of a laser-based deflector. In the first part, we review the basics of the ablation mechanism and build an analytical model based on energetic considerations. This first analytical model allows to predict the efficiency range theoretically allowed by a laser deflection system in absence of rotation. In a second time, we implement a numerical

model to solve the transient heat equation in presence of vaporization and melting and compare the results with respect to the analytical model. The different between the two models allows to draw interesting conclusion regarding the efficiency range of a laser-based deflection system applied to asteroids.

Analytical Steady-State Model:

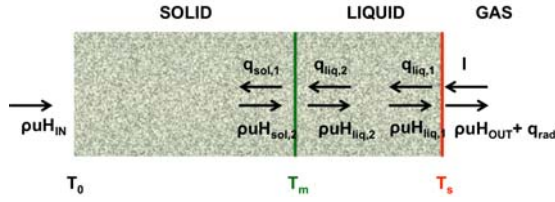


Figure 2: Energy transport during the ablation process

The target considered in this work consists of a rocky S-type asteroid which is conservatively assumed as essentially made of magnesium iron silicates, as they have the highest melting point among the olivine family. Relevant properties of Forsterite, which were retrieved or computed from the data available in the NIST-JANAF thermochemical tables¹ can be reviewed in table 1:

Table 1: Physical properties of Forsterite

Quantity	Symbol	Value
Density	ρ_A	3280 kg/m ³
Thermal Conductivity	k	4.51 W·m ⁻¹ ·K ⁻¹
Heat Capacity (condensed)	c	1464 J·kg ⁻¹ ·K ⁻¹
Thermal Diffusivity	a	0.94 mm ² /s
Vaporization Enthalpy	E_v	14.163 MJ/kg
Melting Enthalpy	E_m	0.508 MJ/kg
reference temperature	T_{ref}	3000K
Saturation pressure (T_{ref})	p_{ref}	4448.9 pa
Melting point	T_m	2171K
Gas Constant	R^*	206.7 J·kg ⁻¹ ·K ⁻¹
Heat ratio (gas)	γ	1.26
Emissivity	ϵ	0.97
Absorptivity	a	0.9
Rest temperature	T_∞	298K

The temperature reached at the ablation front is typically much higher than the triple point of Forsterite (2171K) and therefore the asteroid material undergoes successive phase transformations before reaching the vapour state. A very thin layer of molten material is therefore formed under the ablation front. A simple energy balance allows us to express the energy absorbed by thermal conduction through the different interfaces

¹<http://kinetics.nist.gov/janaf/>

and to derive the continuity relation along the vaporization and melting fronts:

$$q_{liq,1} = aI - q_{rad} - \rho u_v E_v \quad (1)$$

$$q_{liq,2} = q_{sol,1} + \rho u_m E_m \quad (2)$$

The mass flow during the vaporization process is a re-

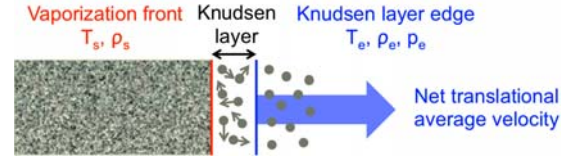


Figure 3: The Knudsen Layer

sult of the thermodynamical non-equilibrium at the interface. As they vaporize, the molecules acquire a net translational velocity component meaning that their distribution function becomes a shifted Maxwellian distribution. The finite layer through which this net velocity can be acquired is called the Knudsen layer and can be treated as a gas-dynamic discontinuity in the equations. The jump conditions have been investigated by Knight [3] and are given in equation 3 :

$$m = \sqrt{\frac{\gamma}{2}} M_e = \frac{v_e}{\sqrt{2R^*T_e}}$$

$$\frac{T_e}{T_s} = \left[\sqrt{1 + \pi \left(\frac{\gamma - 1}{\gamma + 1} \frac{m}{2} \right)^2} - \sqrt{\pi} \frac{\gamma - 1}{\gamma + 1} \frac{m}{2} \right]^2 \quad (3)$$

$$\frac{\rho_e}{\rho_s} = \sqrt{\frac{T_s}{T_e}} \left[\left(m^2 + \frac{1}{2} \right) e^{m^2} \operatorname{erfc}(m) - \frac{m}{\sqrt{\pi}} \right] + \frac{1}{2} \frac{T_s}{T_e} \left[1 - \sqrt{\pi} m e^{m^2} \operatorname{erfc}(m) \right]$$

In this expression, M_e represents the local Mach number on the edge of the Knudsen layer and is dependant on the pressure environment downstream. In vacuum, M_e equates 1 as the flow reaches the sonic limit. The mass flow can thus be computed from equation 3 once the temperature T_s of the interface is known:

$$u(T_s) = \frac{\rho_e(T_s)}{\rho_A} \sqrt{\gamma R^* T_e(T_s)} \quad (4)$$

The liquid near the interface is on the other hand assumed to be near-equilibrium. A Clausius-Clapeyron relation together with the law of perfect gas is used to obtain the dependency between ρ_s and T_s :

$$p_s = \rho_s R^* T_s \quad (5)$$

$$\log \left(\frac{p_s}{p_{ref}} \right) = \frac{E_v}{R} \left(\frac{1}{T_{ref}} - \frac{1}{T_s} \right) \quad (6)$$

Figure 4 represents the interface velocity in function of the surface temperature assuming a sonic ejection velocity.

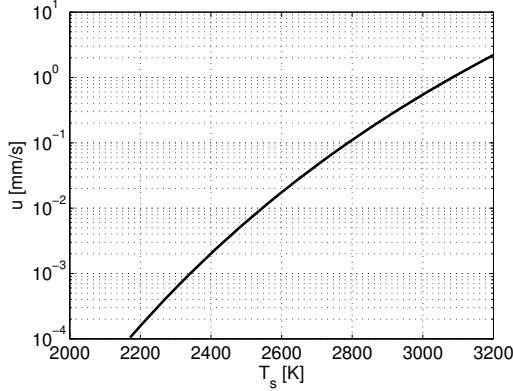


Figure 4: Interface velocity u in function of the surface temperature T_s

In a steady state regime, the internal energy becomes invariant with respect to time, meaning that the heat conducted through the ablation front $q_{liq,1}$ is balanced by the heat required to heat the flow of material crossing it. Therefore, an implicit relation can be found to link the interface temperature to the laser flux I:

$$aI = \epsilon\sigma (T_s^4 - T_\infty^4) + \rho u (E_v + E_m + c(T_s - T_0)) \quad (7)$$

From this temperature, the net force per unit area p_{eff} under the spot is computed by summing the rate of momentum change to the pressure at the edge of the Knudsen layer:

$$\begin{aligned} p_{eff} &= p_e + \rho_e c_e^2 \\ &= (\gamma + 1)p_e \end{aligned} \quad (8)$$

The momentum coupling C_m is defined as the ratio of the force exerted by the power injected. It can also be computed as the ratio of the effective pressure by the power flux:

$$C_m = \frac{p_{eff}}{I} \quad (9)$$

As a result, figure 5 shows the momentum coupling coefficient and surface temperature expected in function of the laser flux. We see that laser ablation is able to produce a thrust around $70\mu N$ per optical watt for fluxes beyond $100MW/m^2$. A minimum flux of about $10MW/m^2$ is required to enable the vaporization process at a meaningful level. The temperature profile can also be computed by solving the steady-state convection-diffusion equation:

$$u \frac{dT}{dz} + \alpha \frac{d^2T}{dz^2} = 0 \quad (10)$$

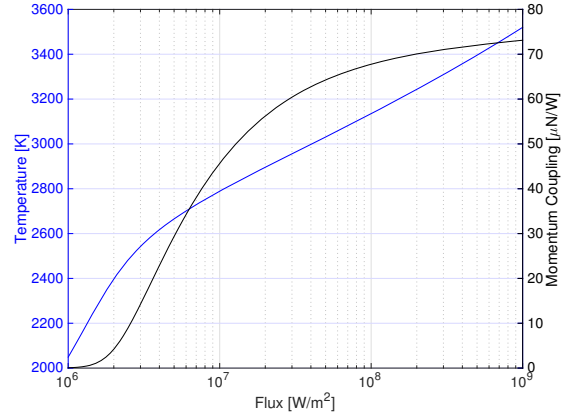


Figure 5: Momentum coupling and surface temperature computed for a range of possible laser fluxes

In this equation, $\alpha = \frac{k}{\rho c}$. The generic solution is on the form $T(z) = A \exp\left(-\frac{u}{\alpha}z\right) + B$. The following boundary conditions are set in the molten and solid phases :

- $T(z = 0) = T_s$
- $T(z = z_m) = T_m$
- $T(z \rightarrow \infty) = T_0$

We thus obtain the following temperature distribution through the condensed phases:

$$T(z) = \frac{T_s - T_m}{1 - \exp\left(-\frac{u}{\alpha}z_m\right)} \exp\left(-\frac{u}{\alpha}z\right) \quad (11)$$

$$+ \frac{T_m - \exp\left(-\frac{u}{\alpha}z_m\right) T_s}{1 - \exp\left(-\frac{u}{\alpha}z_m\right)} \quad \text{if } z < z_m \quad (12)$$

$$= (T_m - T_0) \exp\left(-\frac{u}{\alpha}(z - z_m)\right) + T_0 \quad \text{if } z_m < z$$

The continuity of the conduction flux can then be used to compute the location of the melting front:

$$\frac{ku}{\alpha} \frac{T_s - T_m}{\exp\left(\frac{u}{\alpha}z_m\right) - 1} = \frac{ku}{\alpha} (T_m - T_0) + \rho u E_m \quad (13)$$

By rearranging the terms of equation 13, we find:

$$z_m = \frac{\alpha}{u} \log\left(\frac{T_s - T_m}{T_m - T_0 + \frac{E_m}{c}} + 1\right) \quad (14)$$

Assuming a flux of $39MW/m^2$ such that a temperature of 3000K is reached at the vaporization front, figure 6 shows the resulting temperature distribution in the asteroid material according to equation 11. The characteristic length of the problem is given by $l = \frac{\alpha}{u}$. If we considered that the melting energy is negligible (dotted

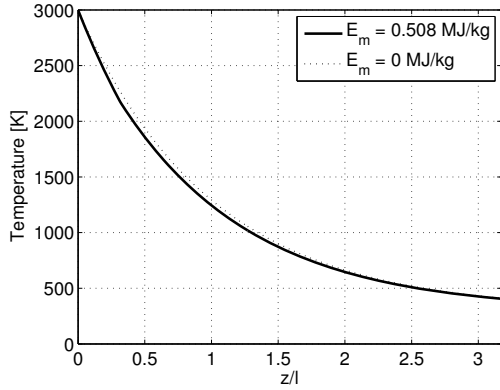


Figure 6: Temperature profile under the laser spot as a function of the normalized distance

line), this length would physically match the intersection of the slope of the temperature profile in $z = 0$ with the horizontal axis $T = T_0$. In other words, this length gives a first order approximation of the distance between the surface and the location where the temperature is equal to the rest temperature T_∞ . A time τ_{ss} to reach the steady-state can also be estimated from the data of the problem [4] and is given by

$$\tau_{ss} = \frac{\alpha}{u^2} \quad (15)$$

The ablation front velocity can be directly computed by equation 4 giving a recession speed of 0.53 mm/s in this case and thus a time to reach the regime-state of about 3.3 seconds. Generally speaking, the front velocity can be roughly estimated from the input power as

$$u \approx \frac{aI}{\rho_A E_v} \quad (16)$$

Therefore, the time to reach the regime-state can be estimated as

$$\tau_{ss} \approx \left(\frac{\Gamma}{aI} \right)^2 \left(\frac{E_v}{c} \right)^2 \quad (17)$$

In which $\Gamma = \sqrt{\rho_a c k}$ is the thermal inertia of the target and the ratio $\frac{E_v}{c}$ has the dimensions of a temperature.

Numerical Transient Model:

A 1D approach is selected as the length of the heated layer is assumed to be smaller than the size of the laser beam and sideways losses can therefore be neglected [5]. Due to the presence of a moving melting front, it is also convenient to write the heat equation in its enthalpy form:

$$\frac{dH}{dt} = -\frac{dq}{dz} + u_s \frac{dH}{dz} \quad (18)$$

Note that the presence of the convective term is due to the fact that we attach the reference frame ($z=0$) at the

ablation front. The heat flux q is expressed through the common Fourier law $q = -k \frac{dT}{dz}$. We divide the material in N control volumes along the direction z . Conservation of the enthalpy for each of these control volumes yields to the discretized form of equation 18:

$$\frac{dH_i}{dt} = -\frac{q_{i+1/2} - q_{i-1/2}}{\Delta z} + u(T_1) \frac{H_{i+1} - H_i}{\Delta z} \quad (19)$$

The fluxes are computed as follows:

$$q_{i+1/2} = -k \frac{T_{i+1} - T_i}{\Delta z} \quad (20)$$

$$q_{i-1/2} = -k \frac{T_i - T_{i-1}}{\Delta z} \quad (21)$$

The temperature is recovered at each time step from the enthalpy which is for convenience defined equal to 0 at the melting temperature:

$$T = T_m + \frac{H}{\rho_A c} \quad \text{if } H \leq 0 \quad (22)$$

$$T_m \quad \text{if } 0 < H < \rho_A E_m \quad (23)$$

$$T_m + \frac{H - \rho_A E_m}{\rho_A c} \quad \text{if } H \geq \rho_A E_m \quad (24)$$

The boundary conditions are then taken into account by setting:

$$q_{1-1/2} = aI - q_{rad}(T_1) - \rho u(T_1) E_v \quad (25)$$

$$q_{N+1/2} = -k \frac{T_\infty - T_N}{\Delta z} \quad (26)$$

Equation 19 is then integrated in Matlab[®] using ode23t which is suitable for moderately stiff problems. As an example, figures 7, 8 and 9 show the evolution of the temperature, enthalpy and momentum coupling with respect to time for an optical flux of 39 MW/m^2 .

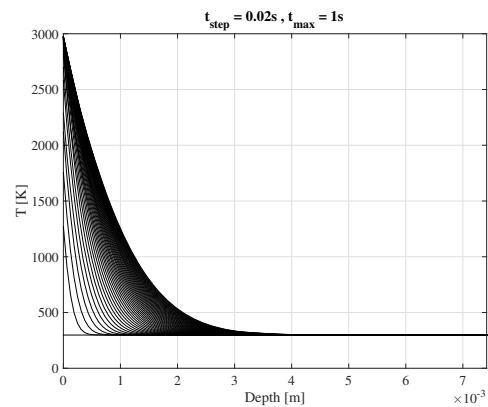


Figure 7: Evolution of the temperature over 1 second considering an optical flux of 39 MW/m^2

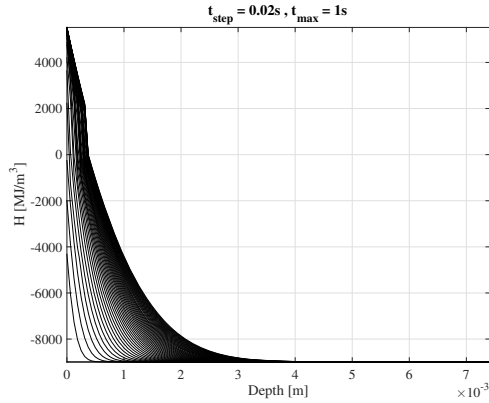


Figure 8: Evolution of the enthalpy over 1 second considering an optical flux of $39\text{MW}/\text{m}^2$

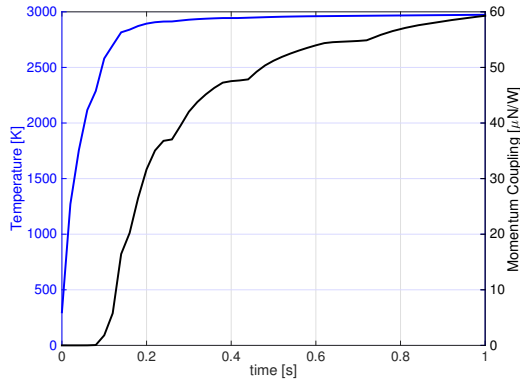


Figure 9: Evolution of the surface temperature and momentum coupling in function of the time considering an optical flux of $39\text{MW}/\text{m}^2$

Effect of the Target Rotation:

The target rotation reduces the time available to heat a given point. Defining $\mathbf{v}_{rot} = \boldsymbol{\omega} \times \mathbf{r}$ the local velocity under the laser spot, the mean time of exposure τ is computed in function of the spot diameter ϕ as

$$\tau = \frac{\pi \phi}{4 v_{rot\perp}} \quad (27)$$

Where the subscript \perp means the transverse direction with respect to the laser beam in the case the exposed surface is inclined. For a given optical flux, the effective momentum coupling is computed by averaging its time evolution during the exposure time τ :

$$\bar{C}_m = \frac{1}{\tau} \int_0^\tau C_m(t) dt \quad (28)$$

Result of the numerical integration of equation 28 is visible on figure 10 for different exposure times in

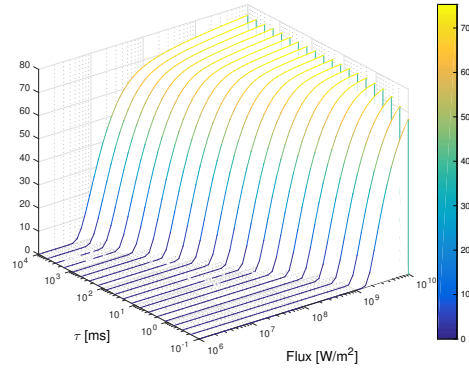


Figure 10: Momentum coupling in function of the mean exposition time τ and the optical flux

function of the optical flux.

Transient effects are seen to shift the region of high efficiency towards higher fluxes while the curve for 10 seconds of mean exposition time appears almost identical to the curve predicted by the steady-state model. Note that the slope of the shift is around -2 in logarithmic scales, which is consistent with the theory developed earlier in which the time to reach the steady-state was predicted to vary in an inverse square fashion with respect to the flux ($\tau_{ss} \propto I^{-2}$). Therefore, both the theory and the numerical model suggest that the impulse coupling is function of the scaling variable $I\sqrt{\tau}$ only. Hence, an asteroid that rotates twice faster will require to multiply the flux by a factor 4 in order to keep the same level of efficiency. Our result is interestingly consistent with studies on pulsed lasers carried out by Phipps et al. [14].

Conclusion:

A new model for the laser deflection of an asteroid has been developed by numerically solving the transient 1D heat equation in presence of vaporization and melting. By comparing the results to an analytical steady state model, we were able to observe the impact on the efficiency of the rotation rate of the asteroid. The rotation rate is inversely proportional to the mean exposition time of the target surface to the laser and therefore a minimum laser flux that depends on this rate is required in order to enable the ablation process. The minimum flux was observed to vary according to the inverse square power of the exposition time, which is in good agreement with the theory. It is worthwhile mentioning that the accuracy of the model is limited by our imprecise knowledge of the physical properties of the asteroid material. In particular, there exists a very scarce knowledge about the optical and thermal conductivity of such

a material in its molten phase. Also, for convenience, we assumed a thermal conductivity, density and heat capacity that was invariant with temperature in our model, considering in each case the worst value possible in the temperature range. The numerical model in equation 19 will be refined in the future to account for the temperature dependency of these quantities. The Saha equation will also be implemented to refine the interface boundary condition and account for the possible formation of plasma at high fluxes.

Acknowledgement: This work is funded by the European Commission's Framework Programme 7, through the Stardust Marie Curie Initial Training Network, FP7-PEOPLE-2012-ITN, Grant Agreement 317185.

References: [1] M. Vasile, et al. (2013) Light touch2: Effective solutions to asteroid manipulation. synova challenge analysis final report *Tech. rep.* University of Strathclyde. [2] A. Gibbings (2012) *Spaceflight*. [3] C. J. Knight (1979) *AIAA journal* 17(5):519. [4] S. I. Anisimov, et al. (1995) *Instabilities in laser-matter interaction* CRC press. [5] S. I. Anisimov, et al. (2002) *Physics-Uspekhi* 45(3):293. [6] P. Sanchez, et al. (2009) *Journal of Guidance, Control, and Dynamics* 32(1):121. [7] R. Kahle, et al. (2006) *Aerospace Science and Technology* 10(3):256. [8] A. L. Gibbings (2014) *Laser ablation for the deflection, exploration and exploitation of near Earth asteroids* Ph.D. thesis University of Glasgow. [9] M. Vasile, et al. (2014) *Acta Astronautica* 103:382. [10] S. Zeidler, et al. (2011) *Astronomy & Astrophysics* 526:A68. [11] T. J. Ahrens, et al. (1972) *The Moon* 4(1-2):214. [12] A. R. Robertson (1968) *JOSA* 58(11):1528. [13] P. Sánchez, et al. (2014) *Meteoritics & Planetary Science* 49(5):788. [14] C. Phipps, et al. (2010) *Journal of Propulsion and Power* 26(4):609.